THE BALD HILLS DOWNBURST

A Thunderstorm Downburst Case Study

by Douglas J. Sherman

DS to Aeronautical Research Laboratories, Victoria, Australia

Presented at the XX OSTIV Congress, Benalla, Australia (1987)

Summary

On November 5, 1977, a weak downburst associated with a multi-cell storm passed over an instrumented tower at Bald Hills, a suburb of Brisbane, Australia. Associated with the thunderstorm was a dome of cold air estimated to be 1200 m to 1800 m deep. Two downdrafts, at least one of which was large enough to be called a downburst, penetrated to the ground near the front edge of this dome. The downburst substantially maintained its vertical velocity down to 100 m above the ground, with one parcel of air having a high vertical velocity and a lateral extent of about 180 m penetrating right down to the 58 m level.

At the 100 m level the vertical downdraft had a peak value of 7.5 m/s and its average value was continuously greater than 4 m/s for at least 50 seconds. The ground wind (measured at 10 m) changed from a north wind of 10 m/s to a south wind of 13 m/s in approximately 90 seconds.

Because of restraint by the surrounding flow, the downdrafts did not spread out as a free wall jet, but as a slower, deeper, submerged jet whose thickness was controlled by downstream conditions. About 1 km ahead of the downburst, and within the cold air flowing away from the storm, was a second gust front which may have been the low level manifestation of the ring vortex which initially surrounds a downburst, and is responsible for the severe horizontal outward flow. Just ahead of this second gust front, and centered at a height of about 50 m, was an indication of a counter-rotating vortex which suggests that the boundary layer of the cold outflow may have separated from the ground, causing the initial ring vortex to lift and so reduce the horizontal outflow wind speeds at ground level.

1. Introduction

A downburst is an intense downdraft and outflow system associated with a thunderstorm. Based on aircraft climb and descent rates, Fujita[1] defined a downburst as a downdraft of 3.6 m/s or more at 90 m above ground. A "microburst" is a small downburst and a "macroburst" is a large one. The demarcation between them depends on the type of observations available. With aircraft encounters in mind Fujita and Caracena[2] specified that the downdraft be 800 m or more in diameter for what would now be called a macrobrust. Subsequently, based on an extensive study of mapped patterns of ground damage, Fujita[3] defined a downburst as being a strong downdraft inducing an outward burst of damaging winds on or near the ground, discriminating between microbursts and macrobursts depending on whether the path length of the damaged area was less or greater than 5 km‡, and showed that for the most common downbursts and microbursts the path width was one half of the past length.

If the upper size limit of a microburst is around 800 m in downdraft diameter, and its path length is 4 to 5 km, associated, on average, with a path width of 2 to 2.5 km, then this suggests that the area of damaging winds commonly extends one downdraft diameter to each side of the downdraft, and the distance travelled by the center of the downburst during its damaging phase is about three downdraft diameters. This indication of downburst proportions is supported by radar observations obtained in Illinois by Project NIMROD[4,5] and near Denver by JAWS[6,7].

In some geographic areas, downbursts are extremely

‡Later Fujita[4] chose a path length of 4 km as the demarcation.

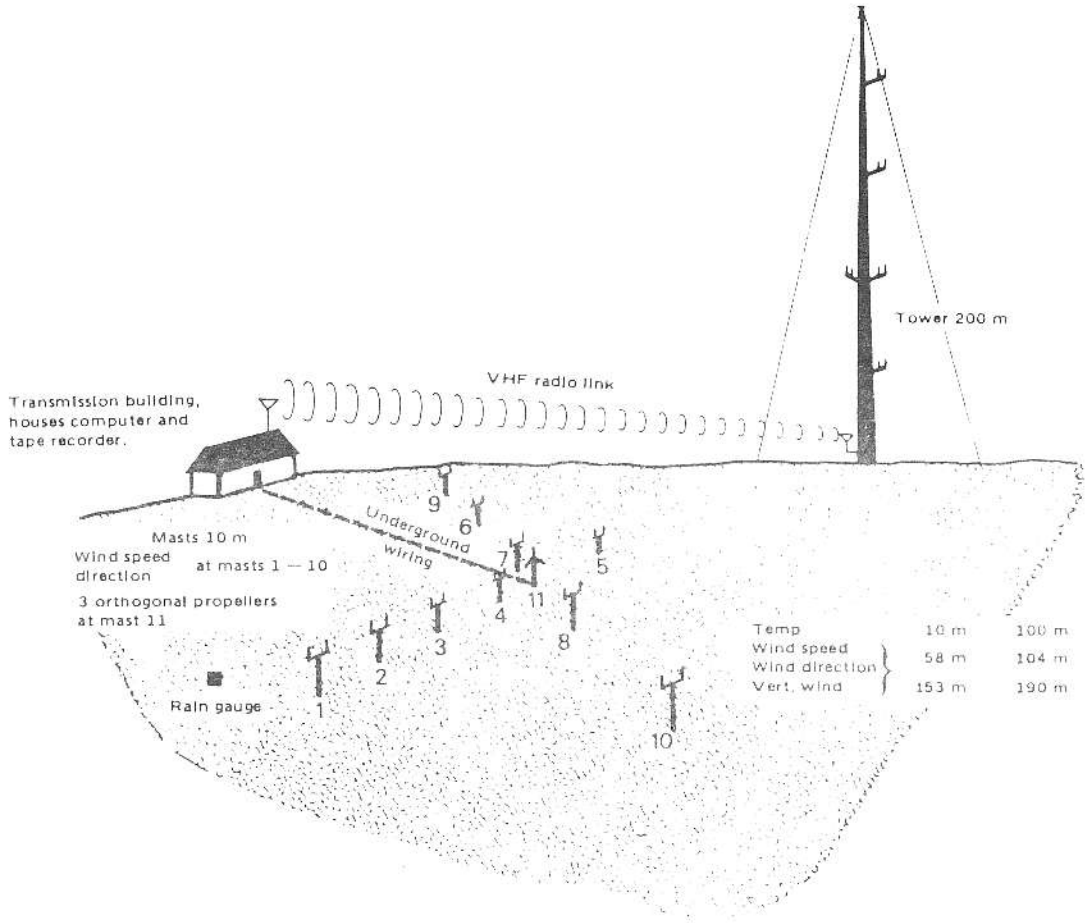

Figure 1. Diagramatic layout of meterological instruments at Bald Hills. Three wind components were measured at approximately 50 m intervals on the 200 m tower, wind speed was measured on each of the 10 m masts numbered 1 to 10 and wind direction was measured at masts 1,3,5,9 and 10. Three wind components at 10 m were measured at mast 11.

common. In a three month season near Boulder, at least 70 microbursts occurred in an area roughly 50 km square. Spillane and Lourensz[8] have estimated that the Sydney airport anemometer experiences an average of 9 downbursts per year with sufficient severity to cause wind shears exceeding an alarm threshold of 15 knots in 1.5 n mi.

Wilson et al[9] indicate that a microburst usually attains its maximum velocity differential within 5 to 10 minutes from reaching the ground, and dissipates in a further 5 minutes. During their descent, and the five minutes or so of strong divergence, downbursts and microbursts may cause severe problems for aircraft,[2-6] but because of their small extent and short life they have rarely been observed at an instrumented tower site. Nevertheless, Goff[10] described the passage of a downburst over a tower in Oklahoma, and this paper will describe the passage of a downburst over an instrumented tower at Bald Hills, a suburb of Brisbane, Australia.

The pressure signal recorded by a microbarograph can be used in some cases to compute a lower bound estimate of the downdraft velocity well above the ground. The stagnation point under the centre of the downdraft causes a pressure rise equal to the dynamic pressure, $q = 0.5\rho w^2$, of the jet. If the jet is travelling past a stationary observer on the ground, the observer will see a pressure spike, which, for a typical thunderstorm downdraft 600 m in diameter travelling at 10 m/s will last for about 60 seconds. Such pressure spikes have sometimes been observed below downbursts, but there have been many downburst passages which have not shown such spikes.

2. The instrumentation system

The Bald Hills tower is a radio transmitting antenna located 20 km north of Brisbane. It was fitted with booms at the heights of 58.2 m, 104.5 m, 153.3 m and 189.9 m to measure the wind speed, direction and vertical wind component.[11] Temperature data are available from the 100 m level, and there was an adjacent array of 10 meter masts on which wind speed and direction were measured (see Figure 1). Data were measured at 1 second intervals and recorded on magnetic tape. Pressure and humidity sensing was not available through the data logging system, but separate chart recorder types of micro-barograph and hygrometer were installed near the transmission building, about 500 m west of the tower.

The site is flat, covered with grass and a few scattered trees. There are clusters of housing about 400 m to the south, and about 800 m to the north-east; otherwise the terrain is open. A WF44 10cm meteorological radar, located near Brisbane airport, is 13.5 km from the tower on a bearing of 153 degrees

(true). At the time of the downburst a Video Integrator Processor (VIP) had been experimentally fitted to the radar to display a maximum of six levels of reflectivity.

3. The data

The downburst passed the tower at 2020 local time on November 5, 1977. Figure 2 shows a series of four radar pictures taken as the center of the isolated storm moved across the site, while Figure 3 shows graphs of a selection of the measured parameters over a one hour period including the incident. The pressure trace from the micro-barograph has been enlarged to the same time scale as the other graphs in Figure 3, although its resolution is poorer and the time synchronisation is subject to possible error (probably less than ± 3 minutes however).

4. The passage of the storm

(a) Radar

The radar sections shown in Figure 2 indicate that the area of the strongest echo was decreasing at the time the storm passed Bald Hills. At the same time, the radar shows the storm top was collapsing at about 2 m/s, indicating the likelihood of strong downdrafts. Moreover, throughout the period, there were portions of the radar echo with reflectivity exceeding 40 dBZ, which indicates the likelihood of severe turbulence.[12] The high reflectivity core is in close proximity to the downdrafts, described below, which passed the tower at 2020.5 and 2021.5.

(b) The gust front and density current outflow

The first effect of the storm on the wind field was at about

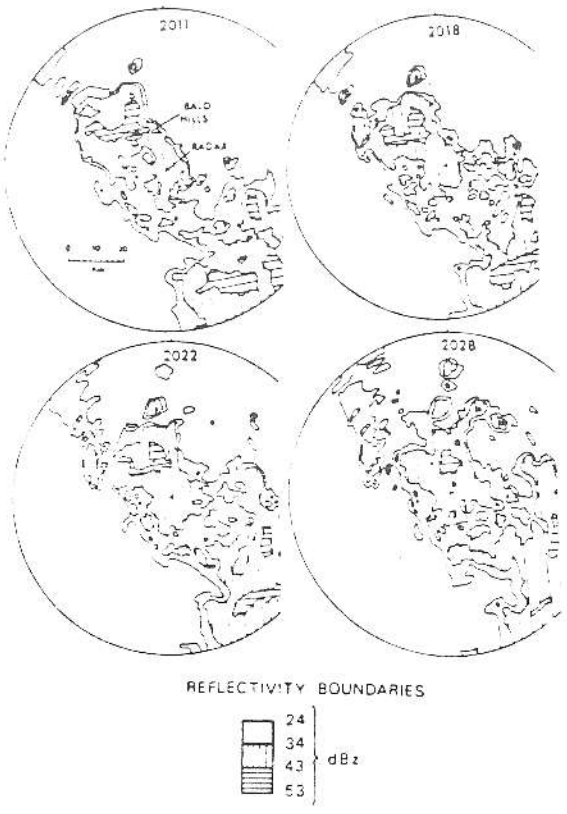

Figure 2. Radar Observations-Brisbane airport, November 5, 1977. PPI radar observations taken with 1.5 degree antenna tilt angle. Times shown are local times.

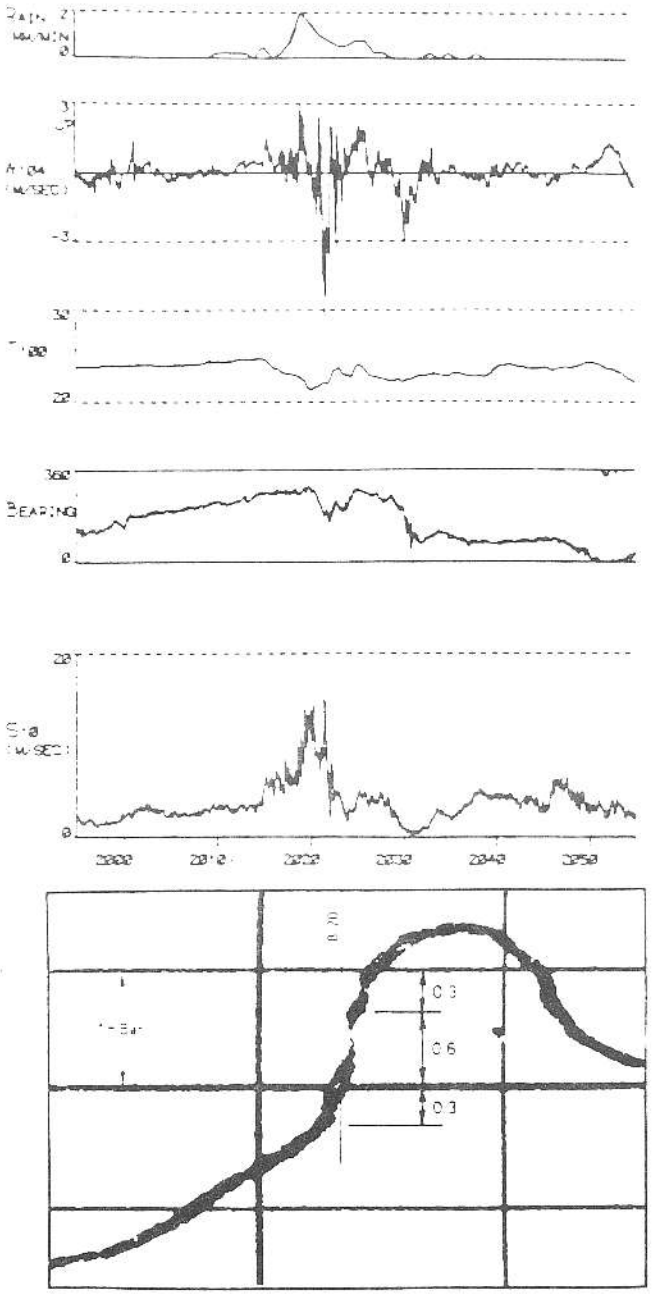

Figure 3. Showing, from bottom to top, graphs of barometric pressure, wind speed and direction at 10 m level, temperature at 100 m level, vertical wind at 104 m level, and rainfall rate during the incident. Temperature, wind direction and speed components are 3-second average values and rainfall rate is 1-minute average value.

2015, when a very mild gust front passed the site. The wind speed at the 58 m and 104 m levels rose from about 6 m/s to 11 m/s with similar but less well defined rises at the other levels, and the temperature dropped from 25 degrees C to 23 degrees C.

Within the density current outflow a second gust front passed the tower at 2019. This was accompanied by a further increase in wind speed (at the 50 m level the rise was most marked from 11 m/s to 18 m/s in 6 seconds), a second zone of uplift and a

further pronounced temperature drop (to 21.5 degrees C). This second gust front was about 90 seconds ahead of the first downdraft. The possible special significance of this second gust front is discussed below.

(c) Downburst flow pattern

The movement of the storm seems, from the radar, to have been approximately from the west with a speed around 12 m/s. To obtain a picture of the air movement relative to the storm, the winds measured by the anemometer array were plotted, as shown in Figure 4, after the vector subtraction of the storm movement velocity, using a space-time transformation.

The vertical profile shows that two separate downdrafts passed the tower. The first downdraft, which passed the tower at 2020.5 did not descend below about the 100 m level. At the section of the tower the horizontal dimension of the downdraft was about 600 m and the mean vertical velocity at the 190 m level was about 2 m/s. It is possible that this downdraft, being at the front of the storm where the newest cells are developing, is in fact a downburst just prior to touch-down. Small advance tongues of the downdraft may have descended right to the ground a little to the north of the tower, because at mast 9, the northernmost mast of the 10 m array, brief episodes of high velocity and rapid wind direction change occurred, indicating the possibility of a small scale (about 50 m) burst swath. The second downdraft, which passed the tower at 2021.5, descended right to the ground. The section through this downdraft at the tower had a horizontal dimension (parallel to the direction of storm motion) of approximately 800 m and a mean downward speed of about 4 m/s. The temperature graph in Figure 3 shows a broad minimum corresponding to the time during which these two downdrafts were passing the tower. There is a rapid rise in temperature after the second downdraft passed, indicating entrainment of warmer air at the rear of this downdraft. The mean downward speed in the second downdraft remained near 4 m/s down to the 100 m level so the second of these downdraft cores may be described as a downburst.

(d) Superimposed wave pattern

The velocity vectors at the 10 m level, plotted in plain view in Figure 4,‡ show that from about 2019 to 2020.5 there is a velocity from the north, reaching approximately 8 m/s at its maximum. This is followed from 2020.5 to 2022 by a velocity from the south which reaches approximately 10 m/s at its maximum. From 2022 to 2024 there is a second surge of wind from the south, reaching approximately 5 m/s for the maximum value of the wind component from the south.

These three surges are not part of the flow pattern moving with the storm, they are an unsteady phenomenon superimposed on the otherwise fairly steady downburst flow pattern. Time histories of the north/south wind component measured at the various anemometers in the horizontal array are shown in Figure 5. If a single event can be traced as it passes over an array, then isochrone plotting will reveal the velocity of translation of the event.

One possible "event" to track across the array is the first maximum in the southerly wind component. These maxima are marked by dots in Figure 5. The isochrones (not illustrated) show that the disturbance comes from the south south-east and travels the 300 m from mast 10 to mast 9 in about 0.4 minutes — giving a propagation speed of about 12.5 m/s. A slightly more difficult "event" to identify is the maximum in the northly wind component around 2020. These maxima are marked by crosses in Figure 5, and the isochrones show that the event comes from the north and travels 250 m or 300 m across the array in some 30 seconds, giving a velocity of propagation around 10 m/s.

(e) The pressure trace

From about 1950 to 2018 the pressure increased, almost linearly with time, by about 1 mb. At 2018 the density current behind the first gust front had completely enveloped the tower and the temperature had stabilised at 23 degrees C. Over the next five minutes the pressure increased rapidly by 1.2 mb. This rapid increase seems to have occurred in three sudden steps of about 0.3, 0.6 and 0.3 mb at about 2018, 2021 and 2023. However, the uncertainty in time synchronization of the pressure trace shown in Figure 3 makes it difficult to associate the pressure steps with specific gust front or downburst events.

After the sudden pressure jumps the pressure remained high for 20 minutes, presumably as a meso-high passed over the site. As the center ofthe meso-high passed, the wind speed fell to nearly zero and another downdraft with a width of the order of 2 km and a mean vertical speed of 1 m/s was observed. Then at 2045 there was a sudden pressure drop of 0.3 mb over a one minute period followed almost immediately by a small rise in wind speed and a 90 degree change in wind direction, possibly where the ambient winds were diverted around the rear of the outflowing air from the downburst.

5. Discussion

(a) The depths of the cold air

Behind the second gust front the temperature fell to 21.5 degrees C, while the ambient air had a temperature of 25 degrees C. The temperature difference of 3.5 degrees C corresponds to a density increase of 0.015 kg/m^3, so the flow depth of a density current causing a 1 mb hydrostatic pressure

‡The velocity vectors, shown in Figure 4, in front of the first downdraft flow away from the storm at all levels except for the 10 m level. This anomaly at the 10 m level is due to the effect of ground friction. The purpose of a space-time transformation is to convert a travelling disturbance (i.e. the storm with its two downdrafts) into a steady flow by imposing a negative velocity equal to the propagation spped of the disturbance (12 m/s). This means that the tower and ground array are envisagred as sweeping to the west, through a stationary storm, as 12 m/s. The ground is imagined to move with the array, and friction drags a layer of air with it. This is the cause of the apparent inflow at the 10 m level despite the outflow at higher levels. (The N-S components of velocity are, however, unaffected.) Close behind the head of the second gust front, at about 2020, the velocities (relative to the moving storm) at the lower levels were approximately:

Surface:	−12 m/s
10 m:	−4 m/s
50 m:	+5 m/s

Thus, the region of reversed flow caused by the presence of the boundary below the density current was approximately 15 m thick and since part of this reversed flow was supplied by air moving forward in the lower levels of the outflow, the total thickness of the friction affected, high, shear, layer was probably at least 20 m.

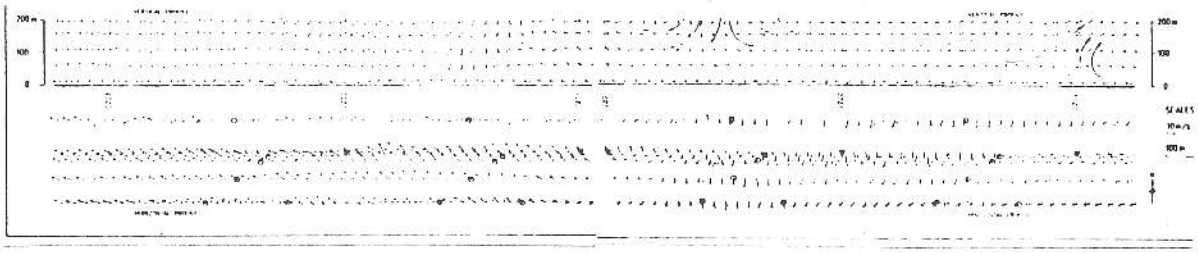

Figure 4. Wind vectors during passage of downdrafts at Bald Hills tower using a space-time transformation. The vertical profile is shown in the upper part of each section of the diagram, and the horizontal profile of winds at the 10 m level is shown in the lower part. Three second average wind vectors are plotted relative to the storm which moved from the west at 12 m/s. In the lower part of each section of the diagram, the position of the tower is marked at 1 minute intervals by a triangle surrounding the origin of the velocity vector. The simultaneous positions of masts 1,3,5,9,10, and 11 in the horizontal array of 10 m masts are indicated by circles.

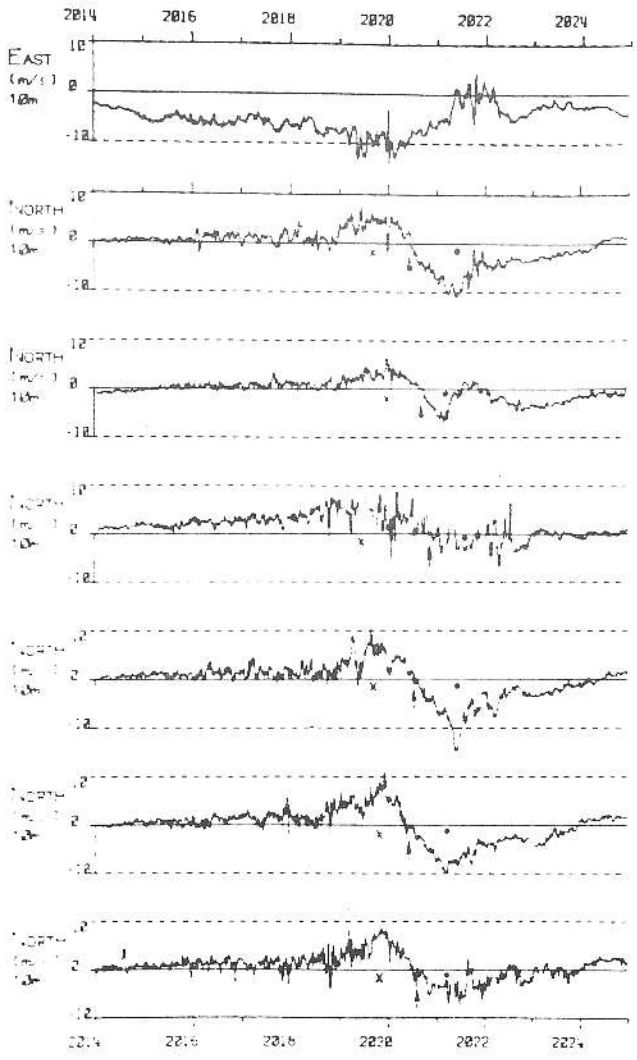

Figure 5. Time histories of northerly wind component measured at various locations in horizontal array. (1 second average values). From the bottom, these graphs are drawn for masts 1,3,5,9,10 and 11. The topmost graph is the component of wind from the east measured at mast 11. The maximum in the northerly wind component is marked with a cross, the zero crossing with an arrow, and the maximum in the southerly wind component is marked with a dot.

rise is 680 m. The dome of cold air covering the site from 2020 to 2045 had a mean temperature of about 23 degrees C, so the pressure excess of about 1 to 1.5 mb during this period corresponds to a cold air depth of about 1200 m to 1800 m.

(b) The possible significance of the second gust front

The downburst and the outflow cannot be distinguished as separate flow phenomena when they are as close as the second gust front is to the two downdrafts. The scaling discussed in the introduction suggests that the important aspects of a downburst, whether considered from the aeronautical or the ground wind viewpoints, are related to the transient phenomena occurring at, and soon after, touch down. At the head of a plume (whether rising light air, as conventionally considered, or falling dense air, as in a downburst) the flow behaves rather like a toroidal vortex. As the vortex approaches the ground, the flow acts as if a mirror image vortex were coming up from below to meet the falling vortex. This mirror image vortex moves each element of the falling vortex outward from the downburst center line so each element follows a roughly hyperbolic path as it approaches the ground surface.

A somewhat similar flow has been observed for the pair of two-dimensional wake vortices behind an aircraft flying close to the ground. There is an increase in the velocities of the fluid near the ground as the vortices approach the ground surface. At first the vortices approach the ground and move apart from each other. However, it has been noted[13,14] that after a short time the vortices reach a minimum altitude and then they rise somewhat. This implies a slowing down of all the velocities associated with them. Harvey and Perry suggest that this rise is associated with the generation of a secondary, counter-rotating, vortex in the boundary layer on the ground. As the vortex makes its initial approach to the ground, it induces increasingly strong velocities on the ground in a direction perpendicular to the vortex axis. Away from the vortex axis the induced velocity decreases, so the developing boundary layer along the ground moves into an adverse pressure gradient. At some stage this adverse pressure gradient is thought to cause boundary layer separation and a secondary counter-rotating vortex which causes the primary aircraft wake vortex (or downburst toroid vortex) to rise away from the ground.

In Figure 4 it may be seen that as a the second gust front passes the tower at 2019 there is a sign of just such a counter-rotating secondary vortex centered at about 50 m. If Harvey and Perry's hypothesis is applicable, then at the stage of the toroid passed the Bald Hills tower it may already have lifted and so terminated the period of intense winds caused by its close proximity to the ground.

(c) The shape of the pressure trace

The flow observed at Bald Hills differed from a simple radial wall jet[15] in that the pressure at the ground jumped to a higher value and stayed high, whereas, on the basis of the simple model, the pressure would be expected to return to its previous value after the jet or downdraft had passed.

A possible explanation in this case is that the dense air behind the downdrafts was not able to flow freely away from the storm. Ground friction and the ambient flow confined the cold air which fell during the previous history of the storm into a dome. The downdrafts were at the front of this dome, and the pressure increase caused by the stagnation at the base of the downdraft was maintained by the hydrostatic pressure of the cold dome. The pressure jumps actually represent sudden jumps in the height of the cold air dome. These cause a horizontal pressure gradient which may partly counteract the falling pressure after the passage of the stagnation point below the axis of the downdraft. The stagnation pressure increase at the base of the downdraft was probably slightly greater than the pressure step due to the increase in height of the cold air because there was still a new flow into the cold air dome.

If, following the description above, of the pressure trace, one of the possible pressure jumps of 0.3 mb is considered to be due to a stagnation pressure increase of $q = 0.5\rho w^2$, it corresponds to a vertical velocity, w, of 7 m/s. The maximum velocity at the 190 m level in the second downdraft just attained 6 m/s which suggests that the pressure transducer may not have been very far off the center of the downburst path.*

(d) The variation of divergence with averaging time and height

For an incompressible fluid the horizontal component of the divergence is given by

$$\frac{\partial u}{\partial x} + \frac{\partial v}{\partial y} = -\frac{\partial w}{\partial z} = -\frac{W}{z}$$

where the second equality is a commonly used approximation, which assumes a linear variation of the vertical velocity component, W, with height, z. This assumption applies for the height averaged value of horizontal divergence over a layer of thickness z, but may not be a good basis for extrapolation to other heights. The peak downward velocity at 10 m altitude (mast 11) was 3.4 m/s, giving a divergence of $3.4/10 = 0.34$/s. This is a very severe divergence but lasted only for 1 second.

The averaging time has considerable effect on the vertical wind component and the divergence. The effects are shown, for the different heights, in Figures 6 and 7. In Figure 6 the maximum value of the N-second average downdraft speed is shown for each value of the averaging time, N, between 1 second and 60 seconds, corresponding to averaging over horizontal spans ranging from 12 m to 720 m. These downdrafts were the maxima observed during the two minute period, starting at 2021, when the second downdraft was passing the tower. The divergences graphed in Figure 7 are simply derived from the downdraft speeds in Figure 6 by dividing by the appropriate height for each case. For the medium term averaging times,

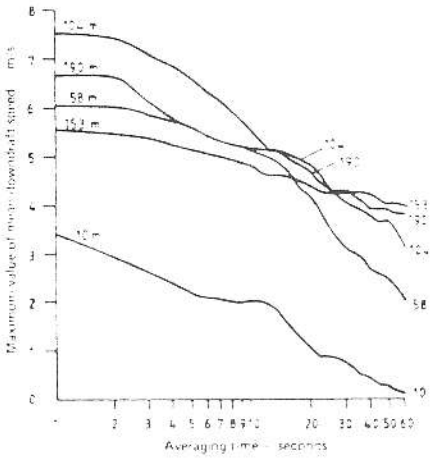

Figure 6. The peak downdraft velocities corresponding to various averaging periods. The velocities are the maximum mean downdrafts observed between 2021 and 2023.

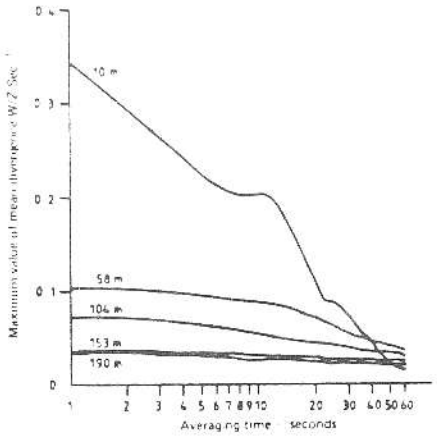

Figure 7. The peak values of divergence corresponding to various averaging periods. Derived from the peak velocities shown in the preceding Figure (Figure 6).

around 10 to 20 seconds, the peak values of the vertical wind speed are approximately the same for all heights except 10 m. This suggests that a peak downdraft parcel of air 180 m wide descended to the 58 m level before being influenced by ground proximity. More generally, parcels seem to be affected by ground proximity at averaging times where the curves in Figure 6 start to drop away from the general average ordinate for the

*The data given by Bradshaw and Love[15] show that the dynamic pressure, q, corresponding to the velocity well above the flat plate falls off with distance from the center line, somewhat faster than the pressure on the flat plate. For example, at the distance $r_{0.5}$ from the center line, the velocity in the absence of the flat plate is, by definition, half that at the center line. The dynamic pressure is one quarter, but the actual pressure excess is 0.4 times that at the center line. A pressure excess measured at a point, X, on the ground away from the center line will thus indicate a velocity greater than that vertically above X but less than that vertically above the stagnation point.

10 to 20 second averaging time, as follows:

Height	Averaging time	Horizontal dimension of parcel
m	sec	m
58	15	180
104	25	300
153	>60	>720

These figures suggest that in modelling the medium scale flow, it may be better to assume that the vertical velocity, rather than the divergence, remains constant with height down to about 50 m or 100 m altitude. In other words, much of the outflow associated with the strongest parts embedded within the downburst occurs below about 50 or 100 m. These features are of the scale of burst swathes — 100 m or 200 m in horizontal extent — so they are significant to property damage, but probably not very significant to powered aircraft. For the very short averaging times (less than 10 second) the peak downdraft speeds *may* rise considerably, but not in any systematic way with altitude. This suggests there are small (approximately 30 m across) parcels of high velocity (possibly significantly colder than average) air embedded in the downdraft. In one passage of a downburst these parcels are encountered randomly by the anemometers at the different heights. (See Figure 6, where the rise of the 1 second average above the 10 second average is much greater at 104 m and 190 m than at 58 m or 153 m.)

An aircraft will experience problems of one type in the falling downdraft well above the ground, and of another type in the region of diverging flow and wind shear adjacent to the ground. A first estimate of the height of transition between these regions can be obtained by examining Bradshaw and Love's variation with height of the pressure excess above a flat plate. When the height above the flat plate is equal to $r_{0.5}$ there is only a small divergence and at 1.5 times this height the divergence is virtually zero. Their transverse variation of dynamic pressure, q, shows that almost all the downdraft is confined within a radius of $1.5r_{0.5}$. The estimated downdraft diameters of 600 m and 800 m suggest that $r_{0.5}$ be taken as 200 m and 270 m respectively, so that, on the basis of the free jet and flat plate model, all of the divergence will occur below levels of 300 to 400 m, with most of the divergence being below 200 to 270 m.

(e) Comparison with the confined outflow

The pattern of velocity vectors in Figure 4 shows a different picture to that inferred from the jet and flat plate model. Before and after the pair of downdrafts, the flow generally is horizontal, directed away from them, and almost constant right up to the highest (190 m) level. There is also the evidence of the pressure jump which suggests cold air to a depth of about 600 m, despite the fact that the downdraft falls to only 100 m above the ground before the vertical velocity at the center line feels much effect from the ground proximity. By comparison the velocity profiles in Bradshaw and Love's outflowing radial wall jet show a pronounced maximum at a fairly low level, and above that the velocity rapidly falls to a low value. The scale height, $d_{0.5}$, for the depth of their wall jet is approximately 0.08 times 1 km (approximately 5 times $r_{0.5}$) from the center of the downburst the scale height (i.e. the height at which the wall jet velocity would be expected to have reduced to 0.5 times the maximum velocity in the local profile) would be only 80 m. This is much smaller than the outflow depth actually observed.

One possible explanation is that Bradshaw and Love used a flat plate of finite extent so that their wall jet could escape and remain free. However, in the atmospheric situation, ground friction and the surrounding flow may confine the cold air in a dome or density current. The wall jet is thus submerged, and although the downburst can penetrate deeply into the dome before they feel the wall effect, they then mix up a deep layer which presumably moves outward over its full depth. The situation is analogous to a stream of water falling into a flat bottomed dish. At first the water rushes outward over the empty bottom in a thin, supercritical, high velocity sheet. But when this water meets the side walls it is dammed up and a hydraulic jump forms. This hydraulic jump moves away from the wall, back towards the jet and eventually merges with the jet. The flow along the base is then a much slower but deeper subcritial flow. This phenomenon provides a possible explanation for the irregular shape of the profiles of vertical velocity. Around both the main downdrafts there were regions of updraft as the flow which fell towards the wall was turned around in a large wave or eddy pattern.

Fujita[3] has remarked that, "although the squall line outflow is deep, often reaching the base of the convective clouds, *the outflow depth of downburst and microbrusts appears to be very shallow.*" (He cited an example of a cellular outflow at Dulles with a depth of 150 m in the head and 100 m behind the head, and a maximum horizontal velocity of 10 m/s.) We thus have two fluid flow phenomena, either or both of which may be involved in explaining these observations. A high momentum jet approaching the ground will tend to behave like Bradshaw and Love's neutrally buoyant, unconfined jet and spread out in a thin high velocity sheet. However, the toroidal eddy at the head may induce an adverse pressure gradient boundary layer which then results in separation and a counter-rotating vortex with a slowing and thickening of the outflow. Moreoever, the outflowing density current establishes a downstream boundary condition governed by the head of the outflow and depending on the rate of inflow into the head and the density difference between the head and the ambient fluid. Once this depth is established the dense fluid builds up behind and submerges the base of the falling downdraft.

(f) Unsteadiness in the downburst flow pattern

In section 4(c), above, it was indicated that unsteady disturbances occurred in the downburst flow pattern. These disturbances took the form of waves of north or south velocity components which moved over the site with wave velocities of the order of 10 m/s. The waves came, approximately, from the north and the south. The velocity of these waves suggest they are gravity waves on the cold air dome, for the velocity, c, of gravity waves on a shallow layer of depth, h, is:

$$c = \left(\frac{gh\Delta\rho}{\rho}\right)^{0.5} = \left(\frac{\Delta p}{\rho}\right)^{0.5}$$

For a pressure excess of 1 to 1.5 mb this gives a wave velocity of 9 to 11 m/s. The actual fluid velocity in the waves is also about $\pm$ 10 m/s, and the complete change from maximum negative to maximum positive velocity occurred in about one or two minutes. Because this change occurred at the time of passage of the downbursts, and with similar scales, it is difficult to separate the magnitudes of the two phenomena. However, the most severe phase of a downburst is unlikely to be affected

severely by such waves because in the early, severe, stages the outflow depth, and hence the wave velocity and probably the scale of fluid velocity in the waves are all much smaller than at later stages. Such waves may represent a significant aeronautical hazard in the interior of a thick gust front flow.

6. Conclusions

In this storm a dome of cold air, estimated to be some 1200 m to 1800 m in thickness, was established during the previous history of the storm. Near the leading edge of this dome two cold downdrafts, at least one of which was big enough to be called a downburst, plunged towards the ground. Peak vertical velocities in the downburst remained nearly constant from 200 m down to 100 m above the ground. The outflow from these downdrafts consisted of a layer about 20 m deep affected by ground friction and above this a layer where the outflow was substantially uniform in the vertical plane to at least the full height of the tower.

From the leading edge of the dome, a density current inferred to be some 700 m thick flowed out about 3 km to a gust front. Behind this first gust front was a second gust front only 1 km from the downbursts. This, second, gust front may be the manifestation of the toroidal vortex which generally forms the head of the descending cold downdraft plume. Closely preceding this second gust front was a counter-rotating vortex centered about 50 m from the ground. This may be attributable to boundary layer separation which has caused the initial toroidal vortex to rise and reduce the horizontal outflow windspeeds on the ground.

Behind the downdrafts the cold air seemed to be at a higher level than in front, for the downdrafts caused a step in the pressure trace rather than a rise and fall. The actual flow pattern in the downbursts was complicated by the presence of disturbances which may have been gravity waves moving on the dome of cold air. These induced velocities which may constitute a hazard for aircraft landing or taking off inside a thick density current or cold air dome.

References

[1]Fujita T.T., 1976: Spearhead echo and downburst near the approach end of John F. Kennedy airport runway, New York City. University of Chicago, SMRP Research Paper, 137 (NTIS Accession No. N76-21841)

[2]Fujita T.T. and F. Caracena, 1977: An analysis of three weather related accidents. Bull Am Met Soc, 58, No 11, 1164-1181.

[3]Fujita T.T., 1978: Manual of downburst identification for project NIM-ROD University of Chicago, SMRP Research Paper, 156 (NTIC Accession NO. N78-30771)

[4]Fujita T.T., 1981: Tornadoes and downbursts in the context of generalized planetary scales. J. Atmos Sci. 38, No 8, 1511-1534

[5]Fujita T.T. and R.M. Wakimoto, 1981: Five scales of airflow associated with a series of downbursts on 16 July 1980. Mon Wea Rev, 109, 1438-1456

[6]Front, W., H.P. Chang, K.L. Elmore and J. McCarthy, 1984: Simulated flight through JAWS wind shear: In-depth analysis results. AIAA 22nd Aerospace Science Meeting, Reno, Nevada, January 1984

[7]Fujita T.T., 1985: The downburst:microburst and macroburst. Report of programs NIMROD and JAWS, SMRP Research Paper, 210, 122pp. (NTIS Accession No PB85-148-880)

[8]Spillane K.T. and R.S. Lourensz, 1986: The hazard of horizontal wind shear to aircraft operations at Sydney Airport. Bureau of Meteorology Research Center, Research Report No. 3, 32pp (Available from BMRC, GPO Box 1289K, Melbourne Vic 3001, Australia)

[9]Wilson J., R. Roberts, C. Kessinger and J. McCarthy, 1984: Microburst wind structure and evaluation of Doppler radar for airport wind shear detection. J. Climate Appl. Meteor., 23, 850-857

[10]Goff R.C., 1982: Characterization of winds potentially hazardous to aircraft. J. Aircraft, 19, No. 2, 151-156

[11]Rider C.K., D.J. Sherman and M.R. Thomson, 1980: Low level wind study. Bald Hills Thunderstorm season 1976-77. Aeronautical Research Laboratories, Melbourne Australia, Structures Report 384. (NTIS Accession No. AD-A108-207)

[12]Lee J.T. and D. Carpenter, 1979: 1973-1977 rough rider turbulence-radar intensity study. Federal Aviation Administration, Report No. FAA-RD-78-115. (NTIS Accession NO. AD-A072-693)

[13]Harvey J.K. and F.J. Perry, 1971: Flowfield produced by trailing vortices in the vicinity of the ground. AIAA Journal, 9, No. 8, 1659-1660

[14]Barker, S.J. and S.C. Crow, 1977: The motion of two-dimensional vortex pairs in a ground effect. J Fluid Mech, 82, part 4, 659-671. (See also Saffman P.G. 1979 J. Fluid Mech, 92, 497-503)

[15]Bradshaw P and E.M. Love, 1961: The normal impingement of a circular air jet on a flat surface. Aeronautical Research Council. Reports and Memoranda, 3205.